The Reactivity of Energetic Materials At Extreme Conditions

L. E. Fried

October 23, 2006

Disclaimer

The Reactivity of Energetic Materials At Extreme Conditions

Laurence E. Fried

Chemistry, Materials Science, and Life Sciences Directorate

Lawrence Livermore National Laboratory

L-282, 7000 East Ave.

Livermore, CA 94550

INTRODUCTION

Energetic materials are unique for having a strong exothermic reactivity, which has made them desirable for both military and commercial applications. Energetic materials are commonly divided into high explosives, propellants, and pyrotechnics. We will focus on high explosive (HE) materials here, although there is a great deal of commonality between the classes of energetic materials. Although the history of HE materials is long, their condensed-phase properties are poorly understood.

Understanding the condensed-phase properties of HE materials is important for determining stability and performance. Information regarding HE material properties (for example, the physical, chemical, and mechanical behaviors of the constituents in plastic-bonded explosive, or PBX, formulations) is necessary for efficiently building the next generation of explosives as the quest for more powerful energetic materials (in terms of energy per volume) moves forward.[1]

In modeling HE materials there is a need to better understand the physical, chemical, and mechanical behaviors from fundamental theoretical principles. Among the quantities of interest in plastic-bonded explosives (PBXs), for example, are thermodynamic stabilities, reaction kinetics, equilibrium transport coefficients, mechanical moduli, and interfacial properties between HE materials and the polymeric binders. These properties are needed (as functions of stress state and temperature) for the development of improved micro-mechanical models,[2] which represent the composite at the level of grains and binder.[3] Improved micro-mechanical models are needed to describe the responses of PBXs to dynamic stress or thermal loading, thus yielding information for use in developing continuum models.

Detailed descriptions of the chemical reaction mechanisms of condensed energetic materials at high densities and temperatures are essential for understanding events that occur at the reactive front under combustion or detonation conditions. Under shock conditions, for example, energetic materials undergo rapid heating to a few thousand degrees and are subjected to a compression of hundreds of kilobars,[4] resulting in almost 30% volume reduction. Complex chemical reactions are thus initiated, in turn releasing large amounts of energy to sustain the detonation process. Clearly, understanding of the various chemical events at these extreme conditions is essential in order to build predictive material models. Scientific investigations into the reactive process have been undertaken over the past two decades. However, the sub-μs time scale of explosive reactions, in addition to the highly exothermic conditions of an explosion, make experimental investigation of the decomposition pathways difficult at best.

More recently, new computational approaches to investigate condensed-phase reactivity in energetic materials have been developed. Here we focus on two different approaches to condensed-phase reaction modeling: chemical equilibrium methods and atomistic modeling of condensed-phase reactions. These are complementary approaches to understanding the chemical reactions of high explosives. Chemical equilibrium modeling uses a highly simplified thermodynamic picture of the reaction process, leading to a convenient and predictive model of detonation and other decomposition processes. Chemical equilibrium codes are often used in the design of new materials, both at the level of synthesis chemistry and formulation.

Atomistic modeling is a rapidly emerging area. The doubling of computational power approximately every 18 months has made atomistic condensed-phase modeling

more feasible. Atomistic calculations employ far fewer empirical parameters than chemical equilibrium calculations. Nevertheless, the atomistic modeling of chemical reactions requires an accurate global Born-Oppenheimer potential energy surface. Traditionally, such a surface is constructed by representing the potential energy surface with an analytical fit. This approach is only feasible for simple chemical reactions involving a small number of atoms. More recently, first principles molecular dynamics, where the electronic Schrödinger equation is solved numerically at each configuration in a molecular dynamics simulation, has become the method of choice for treating complicated chemical reactions.

CHEMICAL EQUILIBRIUM

The energy content of an HE material often determines its practical utility. Accurate estimates of the energy content are essential in the design of new materials[1] and for understanding quantitative detonation tests.[5] The useful energy content is determined by the anticipated release mechanism. Since detonation events occur on a μs timeframe, chemical reactions significantly faster than this may be considered to be in an instantaneous chemical equilibrium. It is generally believed that reactions involving the production of small gaseous molecules (CO_2, H_2O, etc.) are fast enough to be treated in chemical equilibrium for most energetic materials. This belief is based partly on success in modeling a wide range of materials with the assumption of chemical equilibrium[6-8,9].

Unfortunately, direct measurements of chemical species the detonation of a condensed are difficult to perform. Blaise et al[10] have measured some of the species produced in detonating NM using a special mass spectroscopic apparatus. These

measurements pointed to the importance of condensation reactions in detonation. The authors estimate that the hydrodynamic reaction zone of detonating base sensitized liquid nitromethane is 50 μ in thickness, with a reaction time of 7 ns. The hydrodynamic reaction zone dictates the point of which the material ceases to release enough energy to drive the detonation wave forward. Reactions may continue to proceed behind the reaction zone, but the timescales for such reactions are harder to estimate. Typical explosive experiments are performed on parts with dimensions on the order of 1-10 cm. In this case, hydrodynamic confinement is expected to last for roughly a μs, based on a high-pressure sound speed of a several cm/μs. Thus, chemical equilibrium is expected to be a valid assumption for nitromethane, based on the timescale separation between the 7 ns reaction zone and the μs timescale of confinement. The formation of solids, such as carbon, or the combustion of metallic fuels, such as Al, is believed to yield significantly longer timescales of reaction[11]. In this case chemical equilibrium is a rough, although useful, approximation to the state of matter of a detonating material.

Thermodynamic cycles are a useful way to understand energy release mechanisms. Detonation can be thought of as a cycle that transforms the unreacted explosive into stable product molecules at the Chapman-Jouguet (C-J) state[12] (see Fig. 1). This is simply described as the slowest steady-state shock state that conserves mass, momentum, and energy. Similarly, the deflagration of a propellant converts the unreacted material into product molecules at constant enthalpy and pressure. The nature of the C-J state and other special thermodynamic states important to energetic materials is determined by the equation of state of the stable detonation products.
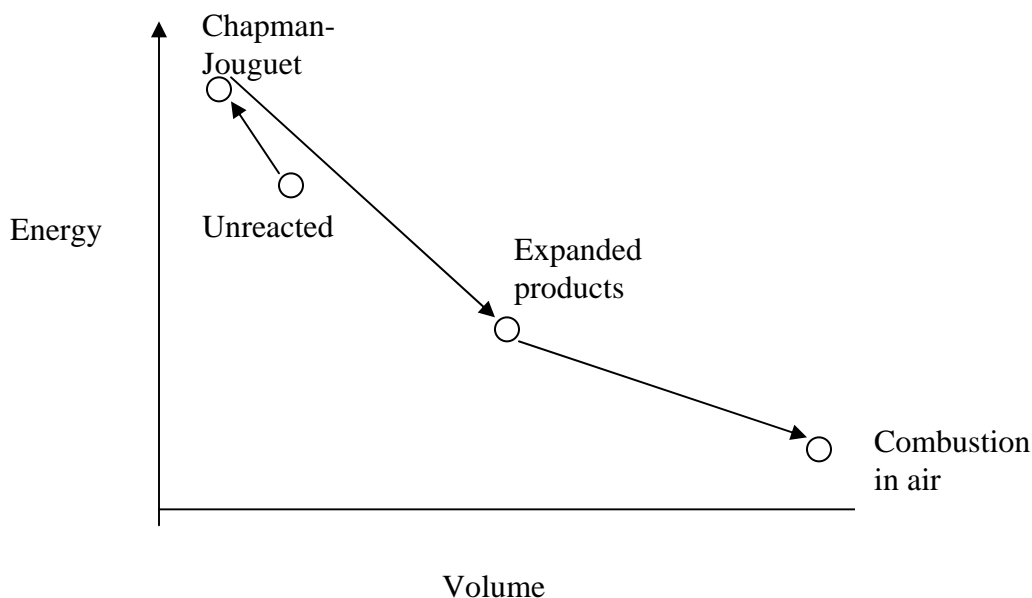
Figure 1: A thermodynamic picture of detonation: the unreacted material is compressed by the shock front and reaches the Chapman-Jouguet point. From there adiabatic expansion occurs, leading to a high volume state. Finally, detonation products may mix in air and combust.

A purely thermodynamic treatment of detonation ignores the important question of reaction time scales. The finite time scale of reaction leads to strong deviations in detonation velocities from values based on the Chapman-Jouguet theory[13]. The kinetics of even simple molecules under high-pressure conditions is not well understood.

High-pressure experiments promise to provide insight into chemical reactivity under extreme conditions. For instance, chemical equilibrium analysis of shocked hydrocarbons predicts the formation of condensed carbon and molecular hydrogen[14]. Similar mechanisms are at play when detonating energetic materials form condensed carbon[8]. Diamond anvil cell experiments have been used to determine the equation of state of methanol under high pressures[15]. We can then use a thermodynamic model to estimate the amount of methanol formed under detonation conditions[16].

6

Despite the importance of chemical kinetic rates, chemical equilibrium is often nearly achieved when energetic materials react. As discussed above, this is a useful working approximation, although it has not been established through direct measurement. Chemical equilibrium can be rapidly reached under high temperature (up to 6000 K) conditions produced by detonating energetic materials[17]. We begin our discussion by examining thermodynamic cycle theory as applied to high explosive detonation. This is a current research topic because high explosives produce detonation products at extreme pressures and temperatures: up to 40 GPa and 6000 K. These conditions make it extremely difficult to probe chemical speciation. Relatively little is known about the equations of state under these conditions. Nonetheless, shock experiments on a wide range of materials have generated sufficient information to allow reliable thermodynamic modeling to proceed.

One of the attractive features of thermodynamic modeling is that it requires very little information regarding the unreacted energetic material. The elemental composition, density, and heat of formation of the material are the only information needed. Since elemental composition is known once the material is specified, only density and heat of formation need to be predicted.

The C-J detonation theory[12] implies that the performance of an explosive is determined by thermodynamic states, the C-J state, and the connected expansion adiabat as illustrated in Fig. 1. The adiabatic expansion of the detonation products releases energy in the form of PV work and heat. Subsequent turbulent mixing of the detonation products in air surrounding the energetic material leads to combustion processes that release more energy.

Thermochemical codes use thermodynamics to calculate states illustrated in Fig. 1, and thus predict explosive performance. The allowed thermodynamic states behind a shock are intersections of the Rayleigh line (expressing conservation of mass and momentum) and the shock Hugoniot (expressing conservation of energy). The C-J theory assumes that a stable detonation occurs when the Rayleigh line is tangent to the shock Hugoniot, as shown in Fig. 2.

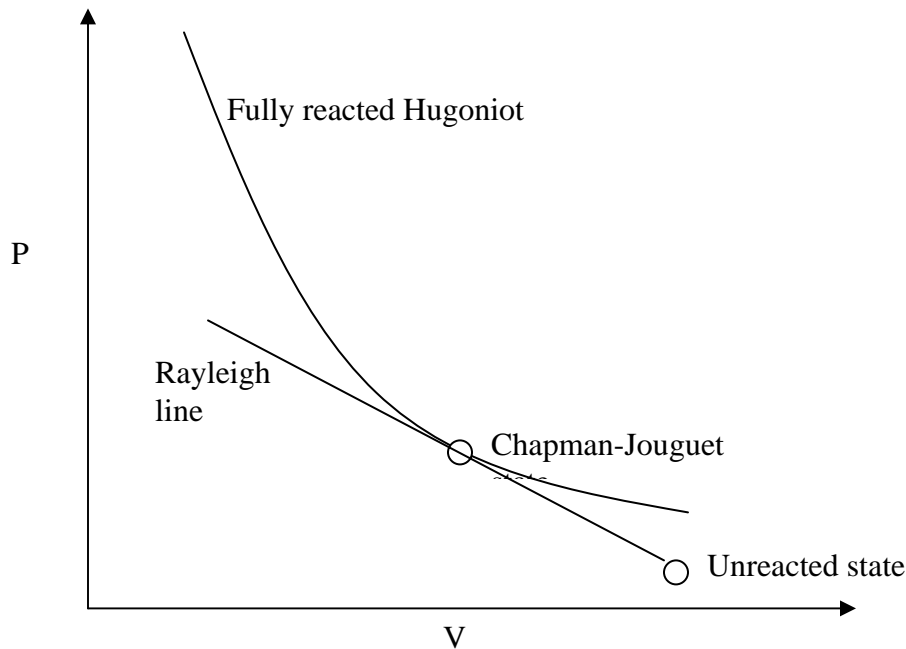**Figure 2: Allowed thermodynamic stated in detonation are constrained to the shock Hugoniot. Steady-state shock waves follow the Rayleigh line.**

This point of tangency can be determined, assuming that the equation of state $P = P(V,E)$ of the products is known. The chemical composition of the products changes with the thermodynamic state, so thermochemical codes must simultaneously solve for state

variables and chemical concentrations. This problem is relatively straightforward, given that the equations of state (EOS) of the fluid and solid products are known.

One of the most difficult parts of this problem is accurately describing the EOS of the fluid components. Because of its simplicity, the Becker-Kistiakowski-Wilson (BKW)[18] EOS is used in many practical energetic material applications. There have been a number of different parameter sets proposed for the BKW EOS.[19] Kury and Souers[5] have critically reviewed these by comparing their predictions to a database of detonation tests. They concluded that BKW EOS does not adequately model the detonation of a copper-lined cylindrical charge. The BKWC parameter set[20] partially overcomes this deficiency through multivariate parameterization techniques. However, the BKWC parameter set is not reliable when applied to explosives very high in hydrogen content.

It has long been recognized that validity of the BKW EOS is questionable[9]. This is particularly important when designing new materials that may have unusual elemental compositions. Efforts to develop better EOS have largely been based on the concept of model potentials. With model potentials, molecules interact via idealized spherical pair potentials. Statistical mechanics is then employed to calculate the EOS of the interacting mixture of effective spherical particles. Most often, the exponential-6 (exp-6) potential is used for the pair interactions:

$$V(r) = \frac{\varepsilon}{\alpha - 6}\left[6\exp(\alpha - \alpha r / r_m) - \alpha(r_m / r)^6\right]$$

Here, r is the distance between particles, r_m is the minimum of the potential well, ε is the well depth, and α is the softness of the potential well.

The JCZ3 (Jacobs-Cowperthwaite-Zwissler) EOS was the first successful model based on a pair potential that was applied to detonation.[21] This EOS was based on fitting

Monte Carlo simulation data to an analytic functional form. Ross, Ree, and others successfully applied a soft-sphere EOS based on perturbation theory to detonation and shock problems.[8,22,23] Computational cost is a significant difficulty with EOS based on fluid perturbation theory. Brown[24] developed an analytic representation of Kang et al.'s EOS using Chebyshev polynomials. The accuracy of the above EOS has been recently evaluated by Charlet *et al*[9].; these authors concluded that Ross's approach is the most reliable. More recently, Fried and Howard[25] have used a combination of integral equation theory and Monte Carlo simulations to generate a highly accurate EOS for the exp-6 fluid.

The exp-6 model is not well suited to molecules with large dipole moments. Ree[7] has used a temperature-dependent well depth $\varepsilon(T)$ in the exp-6 potential to model polar fluids and fluid phase separations. Fried and Howard have developed an effective cluster model for HF.[26] The effective cluster model is valid for temperatures lower than the variable well-depth model, but it employs two more adjustable parameters than does the latter. Jones *et al*.[27] have applied thermodynamic perturbation theory to polar detonation-product molecules. However, more progress needs to be made in the treatment of polar detonation-product molecules.

Efforts have been made to develop EOS for detonation products based on direct Monte Carlo simulations instead of analytical approaches.[28] This approach is promising given the recent increases in computational capabilities. One of the greatest advantages of direct simulation is the ability to go beyond van der Waals 1-fluid theory, which approximately maps the equation of state of a mixture onto that of a single component fluid.[29]

In most cases, interactions between unlike molecules are treated with Lorentz-Berthelot combination rules.[30] These rules specify the interactions between unlike molecules as arithmetic or geometric averages of single molecule pair-interactions. Non-additive pair interactions have been used for N_2 and O_2.[23] The resulting N_2 model accurately matches double-shock data, but is not accurate at lower temperatures and densities.[25] A combination of experiments on mixtures and theoretical developments is needed to develop reliable unlike-pair interaction potentials.

The exp-6 potential has also proved successful in modeling chemical equilibrium at the high pressures and temperatures characteristic of detonation. However, in order to calibrate the parameters for such models, it is necessary to have experimental data for product molecules and mixtures of molecular species at high temperature and pressure. Static compression and sound-speed measurements provide important data for these models.

Exp-6 potential models can be validated through several independent means. Fried and Howard[26] have considered the shock Hugoniots of liquids and solids in the "decomposition regime" where thermochemical equilibrium is established. As an example of a typical thermochemical implementation, we consider the Cheetah thermochemical code[25]. Cheetah is used to predict detonation performance for solid and liquid explosives. Cheetah solves thermodynamic equations between product species to find chemical equilibrium for a given pressure and temperature. From these properties and elementary detonation theory the detonation velocity and other performance indicators are computed.

Thermodynamic equilibrium is found by balancing chemical potentials, where the chemical potentials of condensed species are functions of only pressure and temperature, while the potentials of gaseous species also depend on concentrations. In order to solve for the chemical potentials, it is necessary to know the pressure-volume relations for species that are important products in detonation. It is also necessary to know these relations at the high pressures and temperatures that typically characterize the C-J state. Thus, there is a need for improved high-pressure equations of state for fluids, particularly for molecular fluid mixtures.

In addition to the intermolecular potential, there is an intramolecular portion of the Helmholtz free energy. Cheetah uses a polyatomic model including electronic, vibrational, and rotational states. Such a model can be conveniently expressed in terms of the heat of formation, standard entropy, and constant-pressure heat capacity of each species.

We now consider how the EOS described above predicts the detonation behavior of condensed explosives. The overdriven shock Hugoniot of an explosive is an appropriate EOS test, since it accesses a wide range of high pressures. Overdriven states lie on the shock Hugoniot at pressures above the C-J point (see Fig. 2). The Hugoniot of PETN (penta-erythritol tetranitrate) is shown in Fig. 3. Fried and Howard[31] have calculated the Hugoniot with the exp-6 model and also with the JCZS[32] product library. Good agreement with experiment is found. Since the exp-6 model is not calibrated to condensed explosives, such agreement is a strong indication of the validity of the chemical equilibrium approximation to detonation.
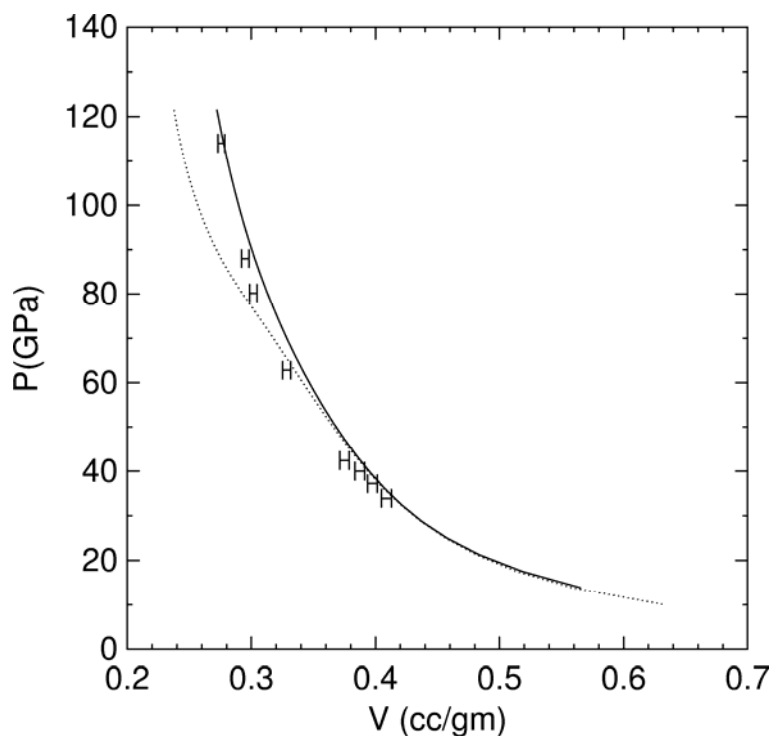
Figure 3. The shock Hugoniot of PETN as calculated with exp-6 (solid line) and the JCZS library (dotted line) vs. experiment (error bars).

Despite the many successes in the thermochemical modeling of energetic materials, there are several significant limitations. One such limitation is that real systems do not always obtain chemical equilibrium during the relatively short (ns-µs) timescales of detonation. When this occurs, quantities such as the energy of detonation and the detonation velocity are commonly predicted to be higher than experiment by a thermochemical calculation.

Chemical kinetic modeling is another possible way to treat detonation. There are several well-developed chemical kinetic mechanisms for highly studied materials such as RDX and HMX[33,34]. Unfortunately, detailed chemical kinetic mechanisms are not

available for high-pressure conditions. Some workers have applied simplified chemical kinetics to detonation processes.[13] The primary difficulty in high-pressure chemical kinetic models is a lack of experimental data on speciation. First principles simulations, discussed below, have the potential to provide chemical kinetic information on fast processes. This information could then conceivably be applied to longer timescales and lower temperatures using high-pressure chemical kinetics.

Finally, there are several issues to be addressed in determining the EOS of detonation products. While convenient, the exp-6 model does not adequately treat electrostatic interactions. In a condensed phase, effects such as dielectric screening and charge-induced dipoles need to be considered. Non-molecular phases are possible under high pressure and temperature conditions. Molecular shape is also neglected in exp-6 models. While the small size of most detonation product molecules limits the importance of molecular shape, lower temperature conditions could yield long-chain molecules, where molecular shape is more important.

The possible occurrence of ionized species as detonation products is a further complication that cannot be modeled using the *exp-6* representation alone. Recent results on the superionic behavior of water at high pressures (see discussion below) provide compelling evidence for a high pressure ionization scenario. These results suggest for example that polar and ionic species interactions may account for approximately 10% of the Chapman-Jouguet (C-J) pressure of PETN. In addition, we note that thermo-chemical calculations of high explosive formulations rich in highly electronegative elements – such as F and Cl, typically have substantially higher errors than calculations performed on

formulations containing only the elements H, C, N, and O. The difficulty in successfully modeling the C-J states of these formulations may be due to the neglect of ionic species.

Bastea et al.[35] have recently extended the exponential-6 free energy approach to include the explicit thermodynamic contributions of the dipolar and ionic interactions. The main task of the new theory is the calculation of the Helmholtz free energy (per particle) of the detonation products – f. The theory starts with a mixture of molecular species whose short range interactions are well described by isotropic, *exp-6* potentials. This includes for example all molecules commonly encountered as detonation products, e.g. N_2, H_2O, CO_2, CO, NH_3, CH_4, etc. As previously documented [36], a one-fluid representation of this system, i.e. replacing the different *exp-6* interactions between species by a single one depending on both individual interactions and mixture composition, is a very good approximation. The authors therefore chose this equivalent system to be the reference, non-polar and neutral one-component *exp-6* fluid. If the mixture components possesses no charge or permanent dipole moments the calculation of the corresponding free energy (per particle) f_{exp-6} suffices to yield the mixture thermodynamics and all desired detonation properties. This has been in fact the physical model previously used in many thermo-chemical codes for the calculation of high explosives behavior.

It is worth noting that at the high pressures and temperatures of interest for detonation the behavior of the *exp-6* fluid so introduced is dominated by short range repulsions and is largely similar to that of a hard sphere fluid. In fact, the variational theory treatment [37] of the *exp-6* thermodynamics employs a reference hard sphere system with an effective, optimal diameter σ_{eff} dependent on density and temperature. Bastea et al. pursued this

connection to the hard sphere fluid by considering first a fluid of equi-sized hard spheres of diameter σ with dipole moments μ. For this simple model of a polar liquid, Stell et. al [38,39] have suggested a Padé approximation approach for the free energy f_d,

$$f_d = f_0 + \Delta f_d$$
$$\Delta f_d = \frac{f_2}{1 - f_3 / f_2}$$

where f_0 corresponds to the simple hard sphere fluid and f_2 and f_3 are terms (second and third order, respectively) of the perturbation expansion in the dipole-dipole interaction $(\sim \mu^2)$

$$f_d = f_0 + f_2 + f_3 + \ldots$$

The first order term f_1 can be shown to be identically zero, while f_2 and f_3 have been explicitly calculated [38]. The resulting thermodynamics can be written in scaled variables as:

$$\Delta f_d = \Delta f_d (\rho^*, \beta_d^*)$$
$$\rho^* = \rho \sigma^3$$
$$\beta_d^* = \frac{\mu^2}{k_B T \sigma^3}$$

where ρ is the (number) density and T is the temperature. The same Padé approximation also holds for a mixture of identical hard spheres with different dipole moments μ_i [40]. We

16

note that under this approximation it is easy to show that the mixture thermodynamics is equivalent with that of a simple hard spheres polar fluid with an effective dipole moment μ given by

$$\mu^2 = \sum_i x_i \mu_i^2$$

where $x_i = \rho_i/\rho$ is the concentration of particles with dipole moment μ_i.

We also adopt the above combination rule for the general case of *exp-6* mixtures that include polar species. Moreover, in this case we calculate the polar free energy contribution Δf_d using the effective hard sphere diameter σ_{eff} of the variational theory.
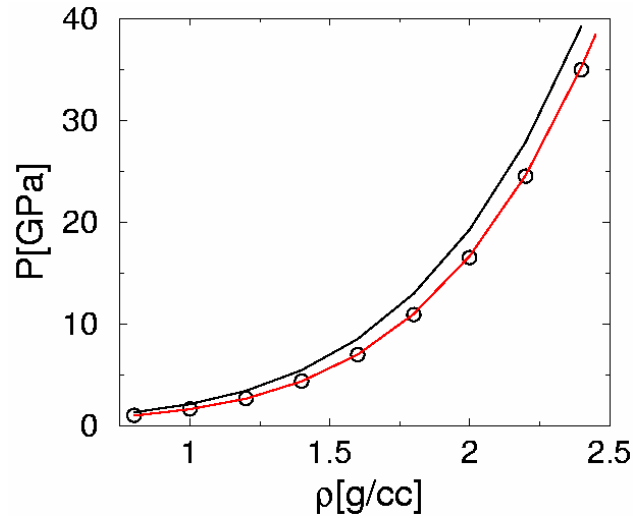

Figure 4: Comparison of pressure results for a model of polar water at T = 2000K: MD simulations (symbols), newly developed theory for polar fluids (red line) and *exp-6* calculations alone (black line).

We show in Figs. 4 and 5 a comparison of this procedure with MD simulation results for an *exp-6* model of polar water. (We also show the results of *exp-6* thermodynamics alone.) For both the pressure and energy the agreement is very good and the dipole moment contribution is sizeable.
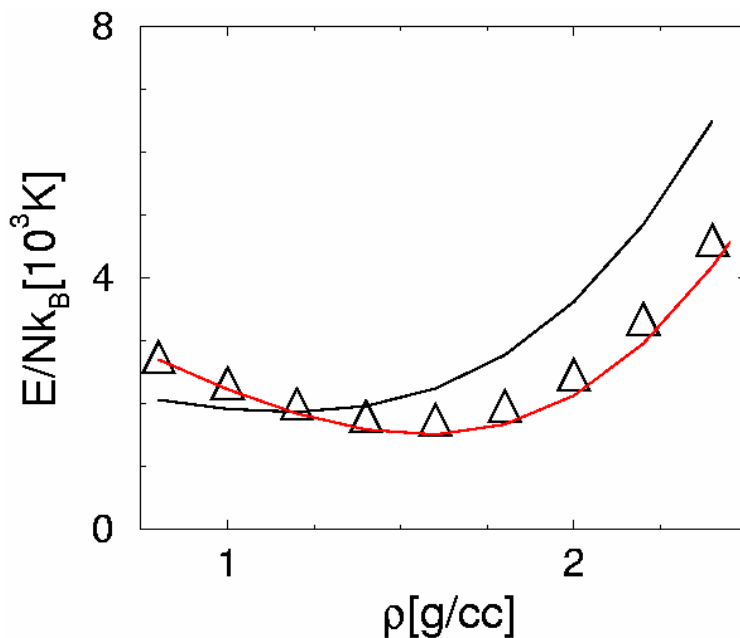

Figure 5: Same as Fig. 1 for energy per particle.

We implemented the thermodynamic theory for *exp-6* mixtures of polar in the thermo-chemical code Cheetah[25]. We considered first the major polar detonation products H_2O, NH_3, CO and HF. We determined the optimal *exp-6* parameters and dipole moment values for these species by fitting to a variety of available experimental data. For water we find for example that a dipole moment of 2.2 Debye reproduces very well all available

experiments. Incidentally, this value is in very good agreement with values typically used to model supercritical water [41].

We show in Fig. 6 a comparison of our Cheetah polar water model predictions with both high pressure Hugoniot data [42], and low density (steam at 800K) experimental data [43]. The agreement is very good for both cases.
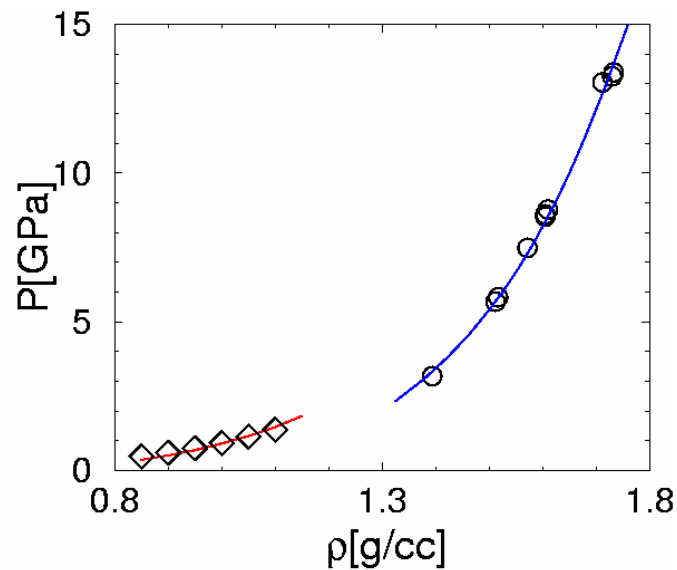

Figure 6: Comparison of theory for polar water: experimental data (Hugoniot – circles and steam at T=800 K – diamonds) and theory (lines).

We applied the newly developed equation of state to the calculation of detonation properties. In this context, one stringent test of any equation of state is the prediction of detonation velocities as a function of initial densities. We choose for this purpose PETN. The results of Cheetah calculations are shown in Fig. 7 along with the experimental data [44]. The agreement is again very good.
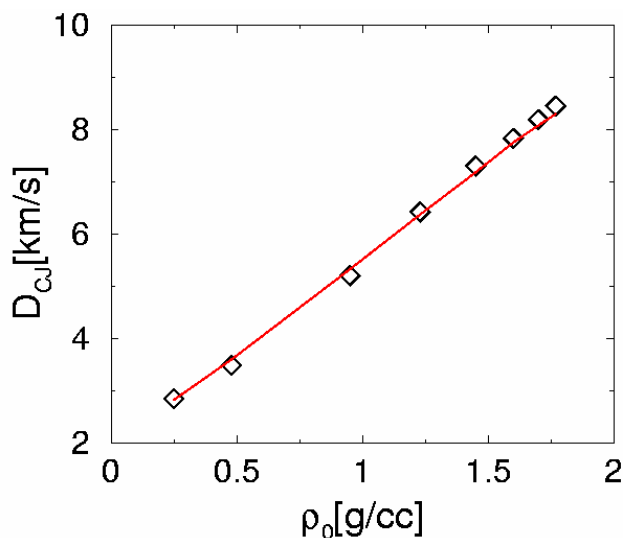
Figure 7: PETN detonation velocity as a function of initial density; experiments (symbols) and CHEETAH calculation (red line).

Advances are continuing in the treatment of detonation mixtures that includes explicit polar and ionic contributions. The new formalism places on a solid footing the modeling of polar species, opens the possibility of realistic multiple fluid phase chemical equilibrium calculations (polar – non-polar phase segregation), extends the validity domain of the previously introduced EXP6 library, and opens the possibility of applications in a wider regime of pressures and temperatures. Predictions of high explosive detonation based on the new approach yield excellent results. A similar theory for ionic species model compares very well with MD simulations, but high explosive chemical equilibrium calculations that include ionization are difficult, due to the presence of multiple minima in the free energy surface. Such calculations will require additional algorithmic developments that we plan to address in the future.

ATOMISTIC MODELING OF CONDENSED-PHASE REACTIONS

Chemical equilibrium methods provide useful predictions of macroscopic detonation processes resultant product molecules. However, no details of the atomistic mechanisms in the detonation are revealed. We now discuss condensed-phase detonation simulations using atomistic modeling techniques. Such simulations are quite useful for understanding the condensed-phase reaction mechanisms on the microscopic level.

Numerous experimental studies have investigated the atomistic details of HE decomposition by examining the net products after thermal (low pressure) decomposition (for example, see Ref.[45]). More specifically for RDX and HMX, the rate limiting reaction is most likely NO_2 dissociation and a plethora of final products in the decomposition process have been isolated. Several theoretical studies have also been reported on the energetics of gas-phase decomposition pathways for HE materials using a variety of methods. For example, we point to work on RDX and HMX where both quantum chemistry[46] and classical simulations of unimolecular dissociation[47] were used.

The gas-phase results provide much insight into the reaction pathways for isolated HE molecules; however, the absence of the condensed-phase environment is believed to strongly affect reaction pathways. Some of the key questions related to condensed-phase decomposition are 1). How do the temperature and pressure affect the reaction pathways? 2). Are there temperature or pressure-induced phase-transitions which play a role in the reaction pathways that may occur? 3). What happens to the reaction profiles in a shock-induced detonation? These questions can be answered with condensed-phase simulations,

but would require large-scale reactive chemical systems (1000s of atoms). Here we present very recent results of condensed-phase atomistic simulations, which are pushing the envelope towards reaching the required simulation goal.

In our group, we are considering whether non-molecular phases of such species could be formed at conditions approaching those of detonation. Condensed phase explosives typically have Chapman-Jouguet pressures in the neighborhood of 20-40 GPa in pressure and 2500-4000K in temperature. Early in the reaction zone, energetic materials are thought to be cooler but more compressed. The Zeldovich-Von Neumann-Doring[48] (ZND) state is defined by the Hugoniot of the unreacted material. This can be probed by shock experiments carefully designed to avoid HE initiation. Estimates of the temperature at the ZND state are in the neighborhood of 1500K, while pressures as high as 60 GPa are possible.

One possible non-molecular phase is a superionic solid. Superionic solids are compounds that exhibit exceptionally high ionic conductivity, where one ion type diffuses through a crystalline lattice of the remaining types. This is a unique phase of matter in which chemical bonds are breaking and reforming very rapidly. Since their discovery in 1836, a fundamental understanding of superionic conductors has been one of the major challenges in condensed matter physics[49]. In general, it has been difficult to create a simple set of rules governing superionic phases. Studies have mostly been limited to metal based compounds, such as metal halides like AgI and PbF_2[49]. However, the existence of superionic solid phases of hydrogen bonded compounds had been theorized previously[50,51].

Recent experimental and computational results indicate the presence of a high pressure triple point in the H_2O phase diagram[52-54], including a so-called superionic solid phase with fast hydrogen diffusion[54,55]. Goldman et al. have recently described the emergence of symmetric hydrogen bonding in superionic water at 2000 K and 95 GPa[55]. In symmetric hydrogen bonding, the intramolecular X-H bond becomes identical to the intermolecular X-H bond, where X is an electronegative element. It has been suggested that for superionic solids a mixed ionic/covalent bonding character stabilizes the mobile ion during the diffusion process[49]. Symmetric hydrogen bonding provides mixed ionic/covalent bonding, and thus could be a key factor in superionic diffusion in hydrogen bonding systems. This represents an entirely novel approach for creating a simple physical description of superionic solids. Due to current limitations in diamond anvil cell techniques, the temperatures and pressures that can be investigated experimentally are too low to probe the role of hydrogen bonding in previously studied hydrides (i.e., H_2O and NH_3). On the other hand, current shock compression experiments have difficulty resolving transient chemical species.

The density profiles of large planets, such as Uranus and Neptune, suggest that there exists within a thick layer of "hot ice", which is thought to be 56% H_2O, 36% CH_4, and 8% NH_3[56]. This has lead to theoretical investigations of the water phase diagram[50], in which Car-Parrinello Molecular Dynamics (CPMD) simulations[57] were conducted at temperature and pressures ranging from 300 to 7000 K and 30-300 GPa[51]. In these first principles molecular dynamics simulations, the electronic degrees of freedom are treated explicitly at each time step, effectively solving the electronic Schrodinger equation at each step. At temperatures above 2000 K and pressures above 30 GPa, there was

observed a superionic phase in which the oxygen atoms had formed a bcc lattice, and the hydrogen atoms diffused extremely rapidly (ca.10^{-4} cm^2/s) via a hopping mechanism between oxygen lattice sites. Experimental results for the ionic conductivity of water at similar state conditions[58,59] agree well with the results from Ref. 3, confirming the idea of a superionic phase, and indicating a complete atomic ionization of water molecules under extreme conditions (P > 75GPa, T > 4000 K)[59].

More recent *ab initio* MD simulations were performed at temperatures up to 2000 K and pressures up to 30 GPa[60]. Under these conditions the authors found that the molecular ions H_3O^+ and OH^- are the major charge carriers in a fluid phase, in contrast to the bcc crystal predicted for the superionic phase. The fluid high pressure phase has been recently confirmed by X-ray diffraction results of water melting at ca. 1000 K and up to 40 GPa pressure[52,61]. In addition, extrapolations of the proton diffusion constant of ice into the superionic region were found to be far lower than a superionic criteria of 10^{-4} cm^2/s.[62]. Thus, it is clear there is great need for further work to resolve the apparently conflicting data.

We have investigated the superionic phase with more extensive first principles Car-Parrinello molecular dynamics simulations[55]. Calculated power spectra (i.e., the vibrational density of states, or VDOS) have recently been compared to measured experimental Raman spectra[54] at pressures up to 55 GPa and temperatures of 1500 K. The agreement between theory and experiment was very good. In particular, weakening and broadening of the OH stretch mode at 55 GPa was found both theoretically and experimentally.

A summary of our results on the phase diagram of water is shown in Figure 8. We find that the molecular to non-molecular transition in water occurs in the neighborhood of the estimated ZND state of HMX. This shows that the detonation of typical energetic materials occurs in the neighborhood of the molecular to non-molecular transition.
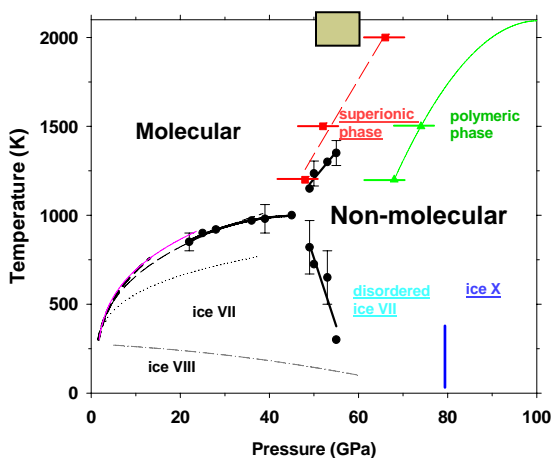

Figure 8: The phase diagram of H$_2$O as measured experimentally[54] (black) and through first principles simulations (red and green colored)[54,55]. The estimated ZND state of HMX is shown as a colored square for reference.

For our simulations, we used the CPMD code v.3.91, with the BLYP exchange-correlation functional[63], and Troullier-Martins pseudo-potentials[64] for both oxygen and hydrogen. A plane wave cutoff of 120 Ry was employed to insure convergence of the pressure, although all other properties were seen to converge with a much lower cutoff (85 Ry). The system size was 54 H$_2$O molecules. The temperature was controlled by using Nosé-Hoover thermostats[65] for all nuclear degrees of freedom. We chose a conservative value of 200 au, and a time step of 0.048 fs.

Initial conditions were generated in two ways: 1) a liquid configuration at 2000 K was compressed from 1.0 g/cc to the desired density in sequential steps of 0.2 g/cc from an equilibrated sample. 2) An ice VII configuration was relaxed at the density of interest, then heated to 2000 K in steps of 300 degrees each, for a duration of 0.5 - 1 ps. While heating, the temperature was controlled via velocity scaling. We will refer to the first set of simulations as the "L" set, and the second as the "S" set. Unless stated otherwise, the results (including the pressures) from the "S" initial configurations are those reported. Once the desired density and/or temperature were achieved, all simulations were equilibrated for a minimum of 2 ps. Data collection simulations were run from 5-10 ps.

The calculated diffusion constants of hydrogen and oxygen atoms are shown in Figure 9, and the inset plot shows the equation of state for this isotherm for both "L" and "S" simulations. The two results are virtually identical up until 2.6 g/cc. At 34 GPa (2.0 g/cc), the hydrogen atom diffusion constant has achieved values associated with superionic conductivity (greater than 10^{-4} cm^2/s). The diffusion constant remains relatively constant with increasing density, in qualitative agreement with the experimental results of Chau et al.[59] for the ionic conductivity.
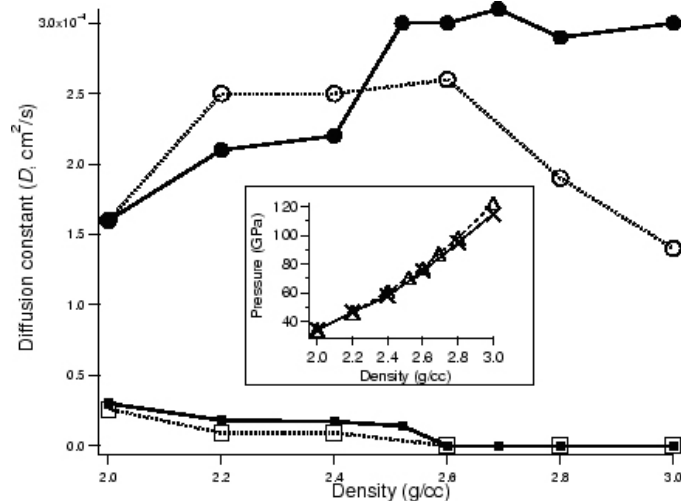
Figure 9: Diffusion constants for O and H atoms at 2000 K as a function of density. The lines with circles correspond to hydrogen and the lines with squares to oxygen. The solid lines correspond to a liquid ("L") initial configuration, and the dashed lines to an ice VII ("S") initial configuration. The inset plot shows the pressure as a function of density at 2000 K, where the triangles correspond to "L" and the X's to "S".

On the other hand, the O diffusion constant drops to zero at 75 GPa (2.6 g/cc) for both "L" and "S" initial configurations. The surprisingly small hysteresis in the fluid to superionic transition allows us to place the transition point between 70 GPa (2.5 g/cc) and 77 GPa (2.6 g/cc). The small hysteresis is most likely due to the weak O-H bonds at the conditions studied, which have free energy barriers to dissociation comparable to k_BT (see below). Simulations which start from the "L" initial configurations are found to quench to an amorphous solid upon compression to 2.6 g/cc.

Our transition pressure of 75 GPa is much higher than the value of 30 GPa predicted earlier[51]. This is likely due to their use of a much smaller basis set (70 Ry). Our results are in disagreement with simple extrapolations of the proton diffusion constant to high temperatures[62].

Radial distribution functions (RDFs) for the "S" simulations are shown in Figure 10. Analysis of the oxygen-oxygen RDF for all pressures yields a coordination number of the first peak of just over 14, consistent with a high density bcc lattice in which the first two peaks are broadened due to thermal fluctuations. The RDF was further analyzed by calculating an "average position" RDF in which the position of each oxygen was averaged over the course of the trajectory. The results for 75 - 115 GPa indicate the

presence of bcc lattice undergoing large amplitude vibrations, even though the RDF's in Figure 10 have width similar to that of a liquid or a glass. The RDFs for the amorphous phase (not shown) are similar to those of the solid phase obtained in the "S" simulations.
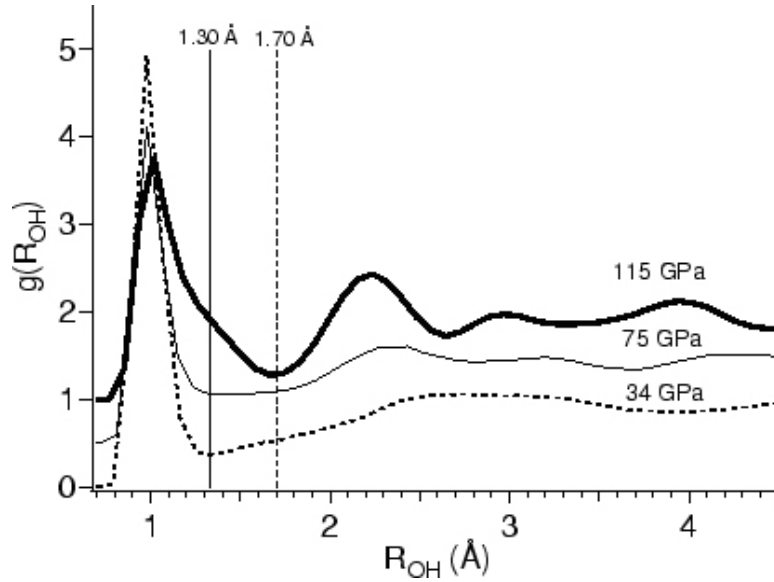

Figure 10: O-H radial distribution function as a function of density at 2000K. At 34 GPa we find a fluid state. At 75 GPa we show a "covalent" solid phase. At 115 GPa, we find a "network" phase with symmetric hydrogen bonding.

The O-O and H-H RDFs (not shown) indicate that no O-O or H-H covalent bonds are formed during the simulations at all densities. The $g(R_{OH})$ shows a lattice-like structure at 115 GPa, which is consistent with proton diffusion via a hopping mechanism between lattice sites[51]. At 34 GPa, the coordination number for the first peak in $g(R_{OH})$ is 2, indicating molecular H_2O. At 95 - 115 GPa, however, the coordination number for the first peak in $g(R_{OH})$ becomes four, indicating that water has formed symmetric hydrogen bonds where each oxygen has four nearest neighbor hydrogens.

Concomitant with this is a shift of the first minimum of the O-H RDF from 1.30Å at 34 GPa to 1.70Å at 115 GPa. We observe a similar structural change in the H-H RDF in

which the first peak lengthens from 1.63Å (close to the result for ambient conditions) to 1.85Å. These observations bear a strong resemblance to the ice VII to ice X transition in which the covalent O-H bond distance of ice becomes equivalent to the hydrogen bond distance as pressure is increased[66]. However, the superionic phase differs from ice X, in that the position of the first peak in $g(R_{OH})$ is not half the distance of the first O-O peak[66]. We analyze the effect of the change in $g(R_{OH})$ below in terms of the molecular speciation in the simulations.

We have determined the free energy barrier for dissociation by defining a free energy surface for the oxygen-hydrogen distances, viz. $W(r) = -k_B T \ln [g(R_{OH})]$ where $W(r)$ is the free energy surface (potential of mean force). The results are shown in Figure 11.
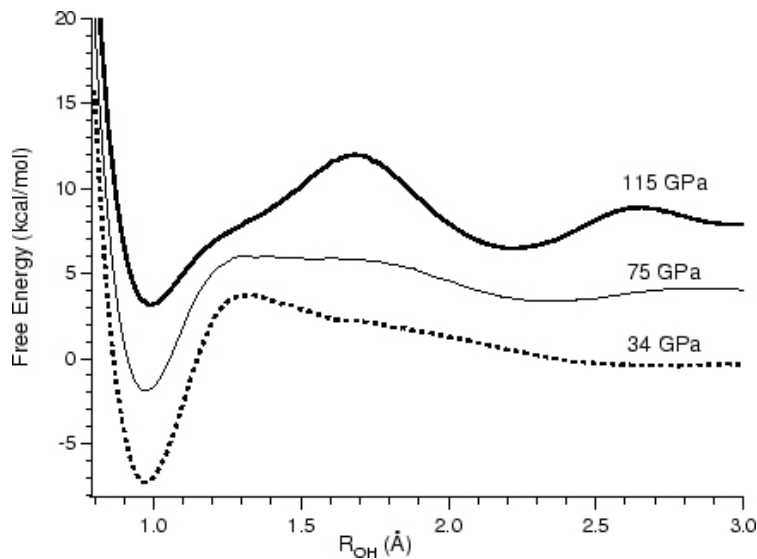

Figure 11: R_{OH} free energy surface at 2000K. The lines are spaced by a factor of 4 kcal/mol for clarity.

The free energy barrier can then be defined as the difference in height between the first minimum and second maximum in the free energy surface. The free energy barrier is 11

kcal/mol at 34 GPa, and 8 kcal/mol at 115 GPa. The remainder of the results discussed below are for the "S" simulations.

We now analyze the chemical species prevalent in water at these conditions. We define instantaneous species based on the O-H bond distance. If the bond distance is less than a value r_c, we count the atom pair as bonded. Determining all the bonds in the system gives the chemical species at each point in time. Species with lifetimes less than an O-H bond vibrational period (10 fs) are "transient", and do not represent bound molecules. The optimal cutoff r_c between bonded and non-bonded species is given by the location of the maximum in the free energy surface[67].

The use of the free energy maximum to define a bond cutoff provides a clear picture of qualitative trends. As expected from the $g(R_{OH})$, at 34 GPa, the free energy peak is found at 1.30Å, which is approximately the same value obtained from simulations of ambient water. At 75 GPa, the free energy peak maintains almost the same position, but broadens considerably. At 115 GPa, the peak has sharpened once again, and the maximum is now at 1.70Å.

Given the above definition of a bond distance, we have analyzed species lifetimes. Above 2.6 g/cc, the lifetime of all species is less than 12 fs, which is roughly the period of an O-H bond vibration (ca. 10 fs). Hence, water above 75 GPa and at 2000 K does not contain any molecular states, but instead forms a collection of short-lived "transient" states. The "L" simulations at 2.6 g/cc (77 GPa) and 2000 K yield lifetimes nearly identical to that found in the "S" simulations described above (within 0.5 fs). This indicates that the amorphous states formed from the "L" simulations are closely related to the superionic bcc crystal states found in the "S" simulations.

Species concentrations are shown in Figure 12. At 34 GPa (2.0 g/cc), H_2O is the predominant species, with H_3O^+ and OH^- having mole fractions of ca. 5%. In addition, some aggregation has occurred in which neutral and ionic clusters containing up to six oxygens have formed. The concentrations of OH^- and H_3O^+ are low for all densities investigated, and non-existent at 95 and 115 GPa (2.8 and 3.0 g/cc). The calculated lifetimes for these species is well below 10 fs for the same thermodynamic conditions (less than 8 fs at 34 GPa). At pressures of 95 and 115 GPa, the increase in the O-H bond distance leads to the formation of extensive bond networks (Figure 13). These networks consist entirely of O-H bonds, while O-O and H-H bonds were not found to be present at any point.
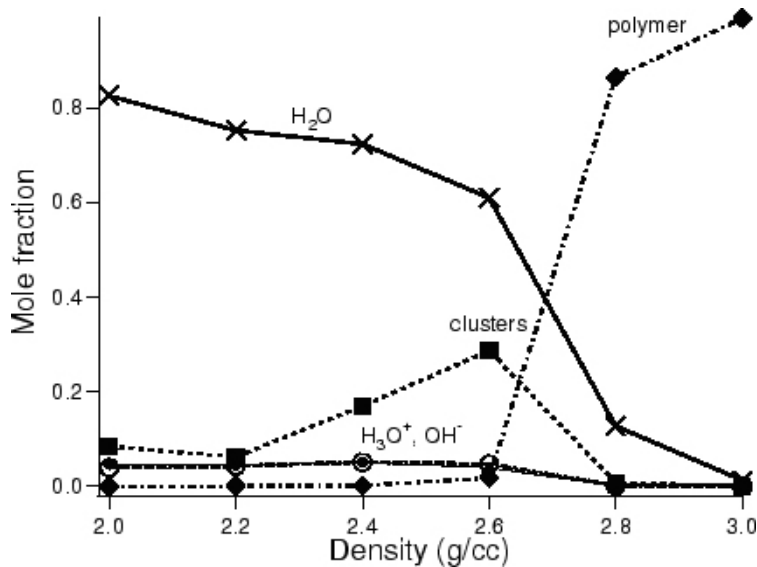

Figure 12: Mole fraction of species found at 34 - 115 GPa and 2000K. The filled circles correspond to H_3O^+, while the open circles to OH^-.
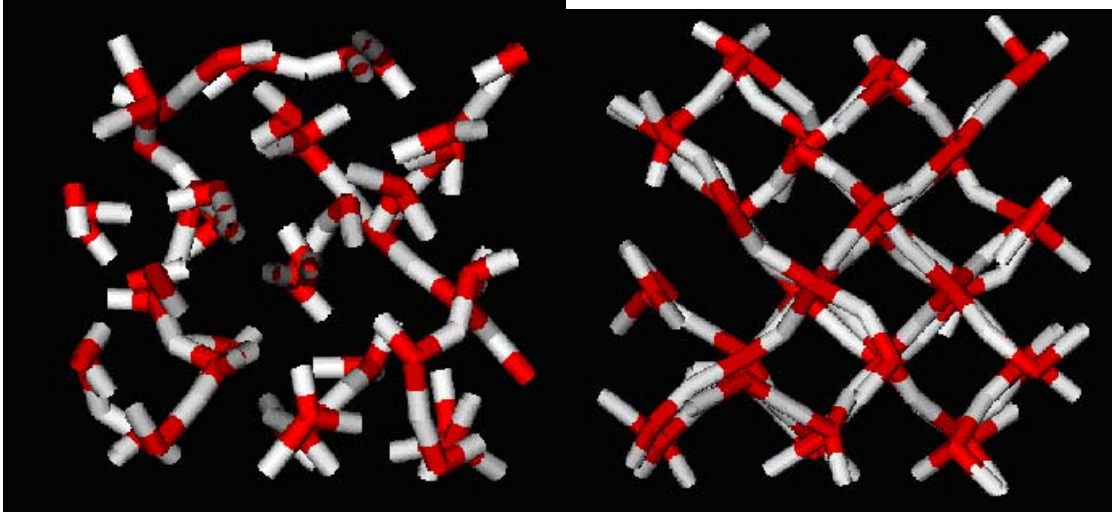
Figure 13: Snapshots of the simulations at 75 GPa and 115 GPa and 2000K. At 75 GPa, the water molecules are starting to cluster, and at 115 GPa, a well defined network has been formed. The protons dissociate very rapidly and form new clusters (at 75 GPa) or networks of bonds (at 115 GPa).

We used Wannier center analysis [68] to compute the percentage of O-H bonds with a Wannier center along the bond axis. Surprisingly, the results for pressures of 34 - 75 GPa consistently showed that 85-95% of the O-H bonds are covalent. For 95 and 115 GPa, we find about 50 - 55% of the bonds are covalent. This is consistent with symmetric hydrogen bonding, for which the split between ionic and covalent bonds would be 50/50. The above simulations show that the molecular to non-molecular transition in H_2O lies just above the operating range of most typical condensed explosives – about 50 GPa. This presents a considerable challenge for thermochemical calculations, since a simple statistical mechanical treatment of non-molecular phases such as superionic water does not yet exist.

FIRST PRINCIPLES SIMULATIONS OF HIGH EXPLOSIVES

Recently, quantum mechanical methods have been applied to systems with up to 1,000 atoms. This is due not only to advances in computer technology, but also improvements in algorithms. A wide range of approximations can also be made to yield a variety of methods; each able to address a different range of questions based on the accuracy of the method chosen. We now discuss a range of quantum mechanical based methods used to answer specific questions regarding shock-induced detonation conditions.

Atomistic simulations have recently been performed on condensed-phase HMX (1,3,5, 7-tetranitro-1, 3,5,7-tetraazacyclooctane). This material is widely used as an ingredient in various explosives and propellants. A molecular solid at standard state, it has four known polymorphs. δ-HMX is believed to be the most highly reactive polymorph. In fact, β-HMX often transforms into δ-HMX before reacting violently[69]. In recent studies, Manaa *et al.*[17] have conducted quantum-based molecular dynamics simulations of the chemistry of HMX and nitromethane[70] under extreme conditions, similar to those encountered at the C-J detonation state.. They studied the reactivity of dense (1.9 g/cm^3) fluid HMX at 3500 K for reaction times up to 55 ps, using the self-consistent charge density-functional tight-binding method (SCC-DFTB). Stable product molecules are formed very rapidly (in a less than one ps) in these simulations. Plots of chemical speciation, however, indicate a time greater than 100 ps is needed to reach chemical equilibrium. Reactions occur very rapidly in these simulations because the system is "pre-heated" to 3500K.In a detonation, on the other hand, a temperature close to 3500K would only be found after stable product molecules had been formed. The initial temperature of unreacted nitromethane after being shocked has been estimated to

be 1800K[10]. HMX likely has a similar initial temperature. Nonetheless, the simulations of Manaa et al. provide useful insight into the chemistry of dense, hot energetic materials. They are a useful complement to more traditional gas phase calculations.

There are numerous experimental characterizations at low temperatures (i.e. < 1000 K, well below detonation temperature) of the decomposition products of condensed-phase HMX.[45,71] These studies tend to identify final gas products (such as H_2O, N_2, H_2, CO, CO_2, etc.) from the surface burn, and the authors aspire to establish a global decomposition mechanism. However, similar experimental observations at detonation conditions (temperatures 2000-5000 K, and pressure 10-30 GPa) have not been realized to date. Computer simulations provide the best access to the short time scale processes occurring in these regions of extreme conditions of pressure and temperature.[72] In particular, simulations employing many-body potentials,[73] or tight-binding models have emerged as viable computational tools, the latter has been successfully demonstrated in the studies of shocked hydrocarbons.[74]

Lewis et al.[75] calculated four possible decomposition pathways of the α-HMX polymorph: N-NO_2 bond dissociation, HONO elimination, C-N bond scission, and the concerted ring fission. Based on the energetics, it was determined that N-NO_2 dissociation was the initial mechanism of decomposition in the gas phase, while they proposed HONO elimination and C-N bond scission to be favorable in the condensed phase. The more recent study of Chakraborty et al.[34] using the density-functional theory (DFT) with B3LYP functionals, reported detailed decomposition pathways of the β-HMX, the stable polymorph at room temperature. It was concluded that consecutive HONO elimination (4HONO) and subsequent decomposition into HCN, OH and NO are

energetically the most favorable pathways in the gas phase. The results also showed that the formation of CH_2O and N_2O could occur preferably from secondary decomposition of methylenenitramine.

The computational approach employed by Manaa *et al*.[17] to simulate the condensed-phase chemical reactivity of HMX is based on implementing the self-consistent charge density-functional tight-binding (SCC-DFTB) scheme.[76] This is an extension of the standard tight-binding approach in the context of DFT that describes total energies, atomic forces, and charge transfer in a self-consistent manner. The initial condition of the simulation included six HMX molecules, corresponding to a single unit cell of the δ phase, with a total of 168 atoms. The density was 1.9 g/cm^3 and the temperature 3500 K in the simulations. These thermodynamic quantities place the simulation in the neighborhood of the C-J state of δ-HMX (3800 K, 2.0g/ cm^3) as predicted through thermochemical calculations. The closest experimental condition corresponding to this simulation would be a sample of HMX, which is suddenly heated under constant volume conditions, such as in a diamond anvil cell. A molecular dynamics simulation was conducted at constant volume and constant temperature. Periodic boundary conditions, whereby a particle exiting the super cell on one side is reintroduced on the opposite side with the same velocity, were imposed.

Under the simulation conditions the HMX was in a highly reactive dense fluid. There are important differences between the dense fluid (supercritical) phase and the solid phase, which is stable at standard conditions. Namely, the dense fluid phase cannot accommodate long-lived voids, bubbles, or other static defects. On the contrary, numerous fluctuations in the local environment occur within a timescale of tens of

femtoseconds (fs). The fast reactivity of the dense fluid phase and the short spatial coherence length make it well suited for molecular dynamics study with a finite system for a limited period of time. Under the simulation conditions chemical reactions occurred within 50 fs. Stable molecular species were formed in less than one ps.

Figure 14 displays the product formation of H_2O, N_2, CO_2 and CO. The concentration, $C(t)$, is represented by the actual number of product molecules formed at time t. Each point on the graphs (open circles) represents an average over a 250 fs interval. The number of the molecules in the simulation was sufficient to capture clear trends in the chemical composition of the species studied. It is not surprising that the rate of H_2O formation is much faster than that of N_2. Fewer reaction steps are required to produce a triatomic species like water, while the formation of N_2 involves a much more complicated mechanism.[33] Further, the formation of water starts around 0.5 ps and seems to have reached a steady state at 10 ps, with oscillatory behavior of decomposition and formation clearly visible. The formation of N_2, on the other hand, starts around 1.5 ps and is still progressing (the slope of the graph is slightly positive) after 55 ps of simulation time, albeit at small variation.
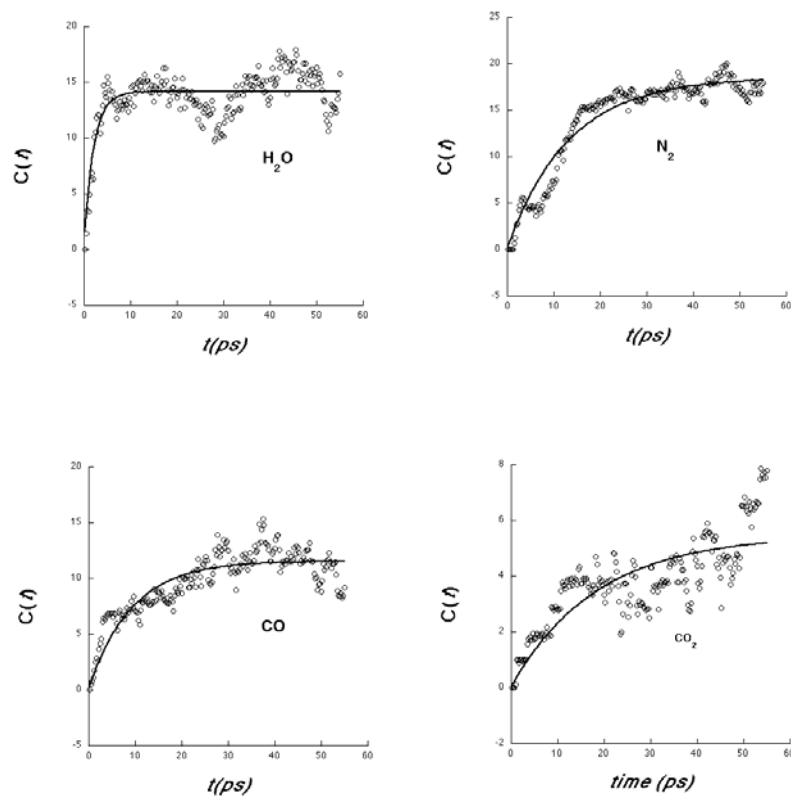
Figure 14: Product particle-number formations as a function of time of H_2O, N_2, CO_2, and CO.

Due to the lack of high-pressure experimental reaction rate data for HMX and other explosives with which to compare, we produce in Fig. 15 a comparison of dominant species formation for decomposing HMX obtained from entirely different theoretical approach. The concentration of species at chemical equilibrium can be estimated through thermodynamic calculations with the Cheetah thermochemical code.[25,77]

As shown in Fig. 15, the results of the MD simulation compare very well with the formation of H_2O, N_2, and HNCO predicted by Cheetah was predicted by the thermochemical calculations. The relative concentration of CO and CO_2, however, is

reversed, possibly due to the limited time of the simulation. In addition, Cheetah predicts that carbon in the diamond phase is in equilibrium with the other species at a concentration of 4.9 mol/kg HMX. No condensed carbon was observed in the simulation. Several other products and intermediates with lower concentrations, common to the two methods, have also been identified. These include HCN, NH_3, N_2O, CH_3OH, and CH_2O. It is hoped that a comparison between the two vastly different approaches can be established at much longer simulation times. In the future, the product-molecule set of the thermochemical code could be expanded with important species determined from ab initio based simulations. It should also be noted that the accuracy of DFT calculations for chemistry under extreme conditions needs further experimental validation.
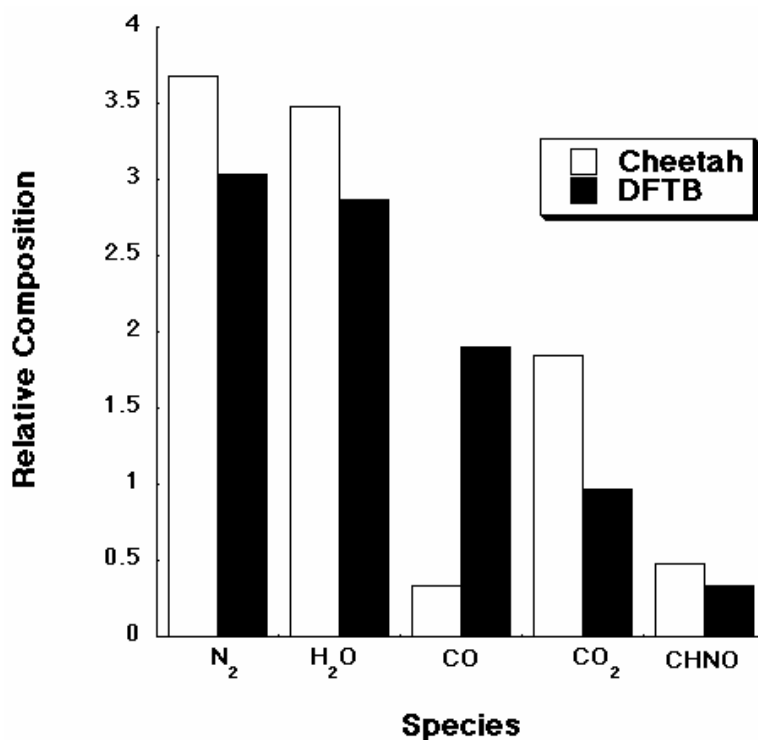

Figure 15: Comparison of relative composition of dominant species found in the MD simulation and in a thermodynamic calculation.

One expects more CO_2 than CO as final products as predicted by Cheetah (Fig. 15), since disproportionation of CO to condensed $C + CO2$ is energetically favorable. The results displayed in Fig. 15 show that at simulation time of 40 ps the system is still in the second stage of reaction chemistry. At this stage the CO concentration is rising and has not yet undergone the water gas shift reaction ($CO + H_2O \rightarrow CO_2 + H_2$) conversion. Interestingly, this shift seems to occur at around 50 ps in the simulation, with CO_2 molecules are being formed while the CO concentration is correspondingly diminishing.

Although the simulation sheds light on the chemistry of HMX under extreme conditions, there are methodological shortcomings that need to be overcome in the future. The demanding computational requirements of the present method limit its applicability to short times and high-temperature conditions. A second issue is that the SCC-DFTB method is not as accurate as high-level ab initio methods. Nonetheless, the present approach could still be considered as a promising direction for future research on the chemistry of energetic materials.

CONCLUSIONS

The ability to model chemical reaction processes in condensed phase energetic materials at the extreme conditions typified by a detonation is progressing. Chemical equilibrium modeling is a mature technique with some limitations. Progress in this area continues, but is hampered by a lack of knowledge of condensed phase reaction mechanisms and rates. A useful theory of the EOS of ionic and highly polar molecular species needs to be more fully developed. The role of unconventional molecular species in detonation needs to be investigated. Finally, high pressure chemical kinetics needs to develop further as a field.

Atomistic modeling is much more computationally intensive, and is currently limited to picosecond time scales. Nonetheless, this methodology promises to yield the first reliable insights into the condensed phase processes responsible for high explosive detonation. Further work is necessary to extend the timescales involved in atomistic simulations. Advanced empirical force fields may offer the ability to model the reactions of energetic materials for periods of many picoseconds. Recent work in implementing thermostat methods appropriate to shocks[78] may promise to overcome timescale limitations in the non-equilibrium molecular dynamics method itself, and allow the reactions of energetic materials to be determined for up to several nanoseconds.

ACKNOWLEDGEMENTS

REFERENCES

1   L. E. Fried, M. R. Manaa, P. F. Pagoria, and R. L. Simpson, Annu. Rev. Mater. Res. **31**, 291 (2001).

2   T. D. Sewell, R. Menikoff, D. Bedrov, and G. D. Smith, J. Chem. Phys. **119** (14), 7417 (2003).

3   I. P. H. Do and D. J. Benson, Int. J. Plasticity **17** (4), 641 (2001); M. R. Baer, Thermochemica Acta **384** (1-2), 351 (2002).

4   Y. B. Zel'dovich and Y. P. Raiser, *Physics of Shockwaves and High Temperature Hydrodynamics Phenomena*. (Academic Press, New York, 1966).

5   P. C. Souers and J. W. Kury, Propellants, Explosives, Pyrotechnics **18**, 175 (1993).

6   M. Cowperthwaite and W. H. Zwisler, J. Phys. Chem. **86**, 813 (1982); W. C. Davis and C. Fauquignon, Journal De Physique IV **5** (C4), 3 (1995).

7   F. H. Ree, J. Chem. Phys. **84**, 5845 (1986).

[8]   M. van Thiel and F. H. Ree, J. Appl. Phys. **62** (5), 1761 (1987).

[9]   F. Charlet, M. L. Turkel, J. F. Danel, and L. Kazandjian, J. Appl. Phys. **84** (8), 4227 (1998).

[10] N. C. Blais, R. Engelke, and S. A. Sheffield, Journal of Physical Chemistry A **101**, 8285 (1997).

[11] M. Cowperthwaite, presented at the Tenth International Detonation Symposium, Boston, Massachusetts, 1993 (unpublished).

[12] W. Fickett and W. C. Davis, *Detonation*. (University of California Press, Berkeley, 1979).

[13] W. M. Howard, L. E. Fried, and P. C. Souers, presented at the 11th International Symposium on Detonation, Snowmass, CO, 1998 (unpublished).

[14] F. H. Ree, J. Chem. Phys. **70** (2), 974 (1979).

[15] J. M. Zaug, L. E. Fried, E. H. Abramson, D. W. Hansen, J. C. Crowhurst, and W. M. Howard, High-Pressure Research **23** (3), 229 (2003).

[16] J. M. Zaug, E. H. Abramson, D. W. Hansen, L. E. Fried, W. M. Howard, G. S. Lee, and P. F. Pagoria, presented at the 12th International Detonation Symposium, San Diego, CA, 2002 (unpublished).

[17] M. R. Manaa, L. E. Fried, C. F. Melius, M. Elstner, and T. Frauenheim, J. Phys. Chem. A **106**, 9024 (2002).

[18] G. B. Kistiakowsky and E. B. Wilson, Report No. OSRD-69, 1941.

[19] M. Finger, E. Lee, F. H. Helm, B. Hayes, H. Hornig, R. McGuire, M. Kahara, and M. Guidry, presented at the Sixth Symposium (International) on Detonation, Coronado, CA, 1976 (unpublished); C. L. Mader, *Numerical modeling of detonations*. (University of California Press, Berkeley, CA, 1979); S. A. Gubin, V. V. Odintsov, and V. I. Pepekin, Sov. J. Chem. Phys. **3** (5), 1152 (1985); M. L. Hobbs and M. R. Baer, presented at the Tenth International Detonation Symposium, Boston, MA, 1993 (unpublished).

[20] L. E. Fried and P. C. Souers, Propellants, Explosives, Pyrotechnics **21**, 215 (1996).

[21] M. Cowperthwaite and W. H. Zwisler, presented at the Sixth Detonation Symposium, 1976 (unpublished).

[22] M. Ross and F. H. Ree, J. Chem. Phys. **73** (12), 6146 (1980); F. H. Ree, J. Chem. Phys. **81** (3), 1251 (1984).

[23] M. van Thiel and F. H. Ree, J. Chem. Phys. **104**, 5019 (1996).

[24] W. Byers Brown, J. Chem. Phys. **87**, 566 (1987).

[25] L. E. Fried and W. M. Howard, J. Chem. Phys. **109** (17), 7338 (1998).

[26] L. E. Fried and W. M. Howard, J. Chem. Phys. **110** (24), 12023 (1999).

[27] H. D. Jones, presented at the Shock Compression of Condensed Matter, 2001, Atlanta, Georgia, 2001 (unpublished).

[28] M. S. Shaw, J. Chem. Phys. **94** (11), 7550 (1991); J. K. Brennan and B. M. Rice, Phys. Rev. E **66** (2), 021105 (2002).

[29] T. W. Leland, J. S. Rowlinson, and G. A. Sather, Trans. Faraday Soc. **64**, 1447 (1947).

[30] T. M. Reed and K. E. Gubbins, *Statistical Mechanics*. (McGraw-Hill, New York, 1973).

31 L. E. Fried, W. M. Howard, and P. C. Souers, presented at the 12 Symposium (International) on Detonation, San Diego, CA, 2002 (unpublished).

32 M. L. Hobbs, M. R. Baer, and B. C. McGee, Propellants, Explosives, Pyrotechnics **24** (5), 269 (1999).

33 C. F. Melius, in *Chemistry and Physics of Energetic Materials*, edited by D. N. Bulusu (Kluwer, Dordercht, 1990).

34 D. Chakraborty, R. P. Muller, S. Dasgupta, and W. A. Goddard III, J. Phys. Chem. A **105**, 1302 (2001).

35 S. Bastea, K. Glaesemann, and L. E. Fried, presented at the 13th Symposium (International) on Detonation, McLean, Virginia, USA, 2006 (unpublished).

36 F. H. Ree, J. Chem. Phys **78**, 409 (1978).

37 M. Ross, J. Chem. Phys. **71**, 1567 (1979).

38 G. Stell, J. C. Rasaiah, and H. Narang, Mol. Phys. **23**, 393 (1972).

39 G. S. Rushbrooke, G. Stell, and J. S. Hoye, Mol. Phys. **26**, 1199 (1973).

40 K. E. Gubbins and C. H. Twu, Chem. Eng. Sci. **33** (1977); C. H. Twu and K. E. Gubbins, Chem. Eng. Sci. **33**, 879 (1977).

41 B. Guillot, J. Mol. Liq. **101**, 219 (2002).

42 S. P. Marsh, *LASL Shock Hugoniot Data*. (University of California Press, Berkeley, 1980).

43 W. Wagner and A. Pruss, J. Phys. CHem. Ref. Data **31**, 387 (2002).

44 H. C. Hornig, E. L. Lee, M. Finger, and J. E. Kurly, presented at the Proceedings of the 5th Symposium (International) on Detonation, 1970 (unpublished).

45 R. Behrens and S. Bulusu, J. Phys. Chem. **95**, 5838 (1991).

46 C. Wu and L. Fried, J. Phys. Chem. A **101** (46), 8675 (1997); S. Zhang and T. Truong, J. Phys. Chem. A **105** (11), 2427 (2001); J. Lewis, K. Glaesemann, K. VanOpdorp, and G. Voth, (2001); D. Chakraborty, R. Muller, S. Dasgupta, and I. W.A. Goddard, J. Phys. Chem. A **105** (8), 1302 (2001).

47 T. Sewell and D. Thompson, J. Phys. Chem. **95** (16), 6228 (1991); C. Chambers and D. Thompson, J. Phys. Chem. **99** (43), 15881 (1995).

48 Y. B. Zeldovich, J. Exp. Theor. Phys. **10**, 542 (1940); A. H. Taub, *J. Von Neumann, Collected Works*. (Pergamon Press, 1963); W. Doring, Ann. Phys. **43**, 421 (1943).

49 S. Hull, Rep. Prog. Phys. **67**, 1233 (2004).

50 P. Demontis, R. LeSar, and M. L. Klein, Phys. Rev. Lett. **60** (22), 2284 (1988).

51 C. Cavazzoni, G. L. Chiarotti, S. Scandolo, E. Tosatti, M. Bernasconi, and M. Parrinello, Science **283**, 44 (1999).

52 B. Schwager, L. Chudinovskikh, A. Gavriliuk, and R. Boehler, J. Phys: Condensed Matter **16**, 1177 (2004).

53 J. F. Lin, E. Gregoryanz, V. V. Struzhkin, M. Somayazulu, H. k. Mao, and R. J. Hemley, Geophys. Res. Lett. **32**, 11306 (2005).

54 A. F. Goncharov, N. Goldman, L. E. Fried, J. C. Crowhurst, I. F. W. Kuo, C. J. Mundy, and J. M. Zaug, Phys. Rev. Lett. **94** (12), 125508 (2005).

55 N. Goldman, L. E. Fried, I. F. W. Kuo, and C. J. Mundy, Phys. Rev. Lett. **94** (21), 217801 (2005).

56 W. B. Hubbard, Science **214**, 145 (1981).

57 R. Car and M. Parrinello, Phys. Rev. Lett. **55** (22), 2471 (1985).

58   W. J. Nellis, N. C. Holmes, A. C. Mitchell, D. C. Hamilton, and M. Nicol, J. Chem. Phys **107** (21), 9096 (1997).

59   R. Chau, A. C. Mitchell, R. W. Minich, and W. J. Nellis, J. Chem. Phys **114** (3), 1361 (2001).

60   E. Schwegler, G. Galli, F. Gygi, and R. Q. Hood, Phys. Rev. Lett. **87** (26), 265501 (2001); C. Dellago, P. L. Geissler, D. Chandler, J. Hutter, and M. Parrinello, Phys. Rev. Lett. **89** (19), 199601 (2001).

61   M. R. Frank, Y. W. Fei, and J. Z. Hu, Geochemica et Cosmochimica Acta **68**, 2781 (2004); J. F. Lin, B. Militzer, V. V. Struzhkin, E. Gregoryanz, and R. J. Hemley, J. Chem. Phys **121**, 8423 (2004).

62   E. Katoh, H. Yamawaki, H. Fujihisa, M. Sakashita, and K. Aoki, Science **295**, 1264 (2004).

63   A. D. Becke, Phys. Rev. A **38**, 3098 (1988); C. Lee, W. Yang, and R. G. Parr, Phys. Rev. B **37**, 785 (1988).

64   N. Troullier and J. Martins, Phys. Rev. B **43**, 1993 (1991).

65   S. Nosé, Mol. Phys. **52**, 255 (1984).

66   M. Benoit, A. H. Romero, and D. Marx, Phys. Rev. Lett. **89**, 145501 (2002).

67   D. Chandler, J. Chem. Phys. **68** (6), 2959 (1978).

68   P. L. Silvestrelli and M. Parrinello, Phys. Rev. Lett. **82**, 3308 (1999).

69   A. G. Landers and T. B. Brill, J. Phys. Chem. **84**, 3573 (1980).

70   M. R. Manaa, E. J. Reed, L. E. Fried, G. Galli, and F. Gygi, J. Chem. Phys **120** (21), 10145 (2004).

71   B. Suryanarayana, R. J. Graybush, and J. R. Autera, Chem. Ind. London **52**, 2177 (1967); S. Bulusu, T. Axenrod, and G. W. A. Milne, Org. Mass. Spectrom. **3**, 13 (1970); M. Farber and R. D. Srivastava, presented at the 16th JANNA Combus. Meeting, 1979 (unpublished); C. V. Morgan and R. A. Bayer, Combust. Flame **36**, 99 (1979); R. A. Fifer, in *Progress in Astronautics and Aeronautics*, edited by K. K. Kuo and M. Summerfield (AIAA Inc., New York, 1984), Vol. 90, pp. 177; R. Behrens, Int. J. Chem. Kinet. **22**, 135 (1990); J. C. Oxley, A. B. Kooh, R. Szekers, and W. Zhang, J. Phys. Chem. **98**, 7004 (1994); T. Brill, P. Gongwer, and G. Williams, J. Phys. Chem. **98** (47), 12242 (1994); T. B. Brill, J. Prop. Power **11**, 740 (1995); C.-J. Tang, Y. J. Lee, G. Kudva, and T. A. Litzinger, Combust. Flame **117**, 170 (1999).

72   P. Politzer and S. Boyd, Struct. Chem. **13**, 105 (2002).

73   C. T. White, D. H. Robertson, M. L. Elert, and D. W. Brenner, in *Microscopic Simulations of Complex Hydrodynamic Phenomena*, edited by M. Mareschal and B. L. Holian (Plenum Press, New York, 1992), pp. 111; D. W. Brenner, D. H. Robertson, M. L. Elert, and C. T. White, Phys. Rev. Lett. **70**, 2174 (1993); M. L. Elert, S. V. Zybin, and C. T. White, J. Chem. Phys. **118**, 9795 (2003).

74   S. R. Bickham, J. D. Kress, and L. A. Collins, Journal of Chemical Physics **112**, 9695 (2000); J. D. Kress, S. R. Bickham, L. A. Collins, B. L. Holian, and S. Goedecker, Physical Review Letters **83**, 3896 (1999).

75   J. Lewis, T. Sewell, R. Evans, and G. Voth, J. Phys. Chem. B **104** (5), 1009 (2000).

76   M. Elstner, D. Porezag, G. Jungnickel, J. Elsner, M. Hauk, T. Frauenheim, S. Suhai, and G. Seifert, Physical Review B **58**, 7260 (1998).

[77]   L. E. Fried and W. M. Howard, Phys. Rev. B **61** (13), 8734 (2000).

[78]   E. J. Reed, J. D. Joannopoulos, and L. E. Fried, Phys. Rev. Lett. **90** (23), 235503 (2003); J. B. Maillet, M. Mareschal, L. Soulard, R. Ravelo, P. S. Lomdahl, T. C. Germann, and B. L. Holian, Phys. Rev. E **63** (1), 016121 (2001).